Proceedings of the Anatomical Society of Great Britain and Ireland

FEBRUARY 1966

An Ordinary Meeting of the Society for the Session 1965–66 was held on Friday 25 February 1966 at the Department of Anatomy, University College, London.

The President (Professor D. V. Davies) and Professor J. Z. Young occupied the Chair at the various sessions.

The following are the authors' abstracts of papers presented.

One hundred years after Grandry. By T. A. QUILLIAM. *University College London* (Fig. 1)

On morphological grounds, encapsulated receptors (i.e. corpuscles) may be conveniently grouped into either lamellated or non-lamellated categories. In general, the appearances presented by each individual variety, when studied either by conventional light, phase or electron microscopy, are complimentary.

In all cases, the nerve terminal itself is unmyelinated and bare of a recognizable Schwann cell sheath. In most lamellated corpuscles the terminal is single, straight and comparatively broad but in many non-lamellated corpuscles the terminal, though usually linear, is thin and convoluted and may be branched or even multiple.

The lamellated receptors are maximally sensitive to vibration over specific frequency ranges but the physical parameters of the stimuli to which the non-lamellated corpuscles respond are not nearly so well defined.

Recently, considerable interest has been focused on the non-lamellated corpuscle first described almost exactly a century ago by Grandry and subsequently named after him (Ciba Foundation Symposium *Heat, Touch and Pain*, 1965). Many hundreds of these corpuscles form one phase of the binary receptor array situated in the dermis of the duck bill. In silver stained sections (Fig. 1 A) the nerve terminal takes the unusual form of a fan shaped reticulum. Yet, in unstained phase (Fig. 1 B) or electron microscope preparations (Fig. 1 C), the terminal almost invariably appears linear in form, being about 2 μm wide by 40 μm long. It is packed with mitochondria and possesses many large and small vesicles. It lies between two satellite cells containing numerous mitochondria which tend to congregate near the terminal and innumerable small, randomly distributed, osmophilic, membrane bounded globules. Peripherally, these latter may be grouped together in subpopulations of 20–40, so that although few of the individual globules exceed 150 mμm in diameter, their corporate presence is reflected in the granular cytoplasmic pattern of the satellite cells seen in light microscopy. Cytoplasmic fibrils and granular and agranular vesicles are also present and finger-like processes project into, and interdigitate with, the capsule complex.

Electron microscopy of degeneration in the prepyriform cortex. By L. E. WESTRUM. *University College London and U.S. Public Health Service* (Fig. 2)

The molecular layer of the prepyriform cortex in rats was studied with the electron microscope, both in the normal and after unilateral olfactory bulb removals ranging from 6 h to 3 months. The material was fixed by immersion or perfusion and double stained (Westrum, *J. Miscrocop.* **4**, 1965).

Normal synapses in this area are predominantly axo-dendritic, occurring on dendritic shafts, their swellings or on spines of various types. Many of the synapses have intricate

interdigitations of the pre- and post-synaptic processes. The contacts are usually of Gray's type 1 but the synaptic thickenings are of varying length.

Degenerative changes in the synaptic bags occur between 18 and 24 h after the lesion.

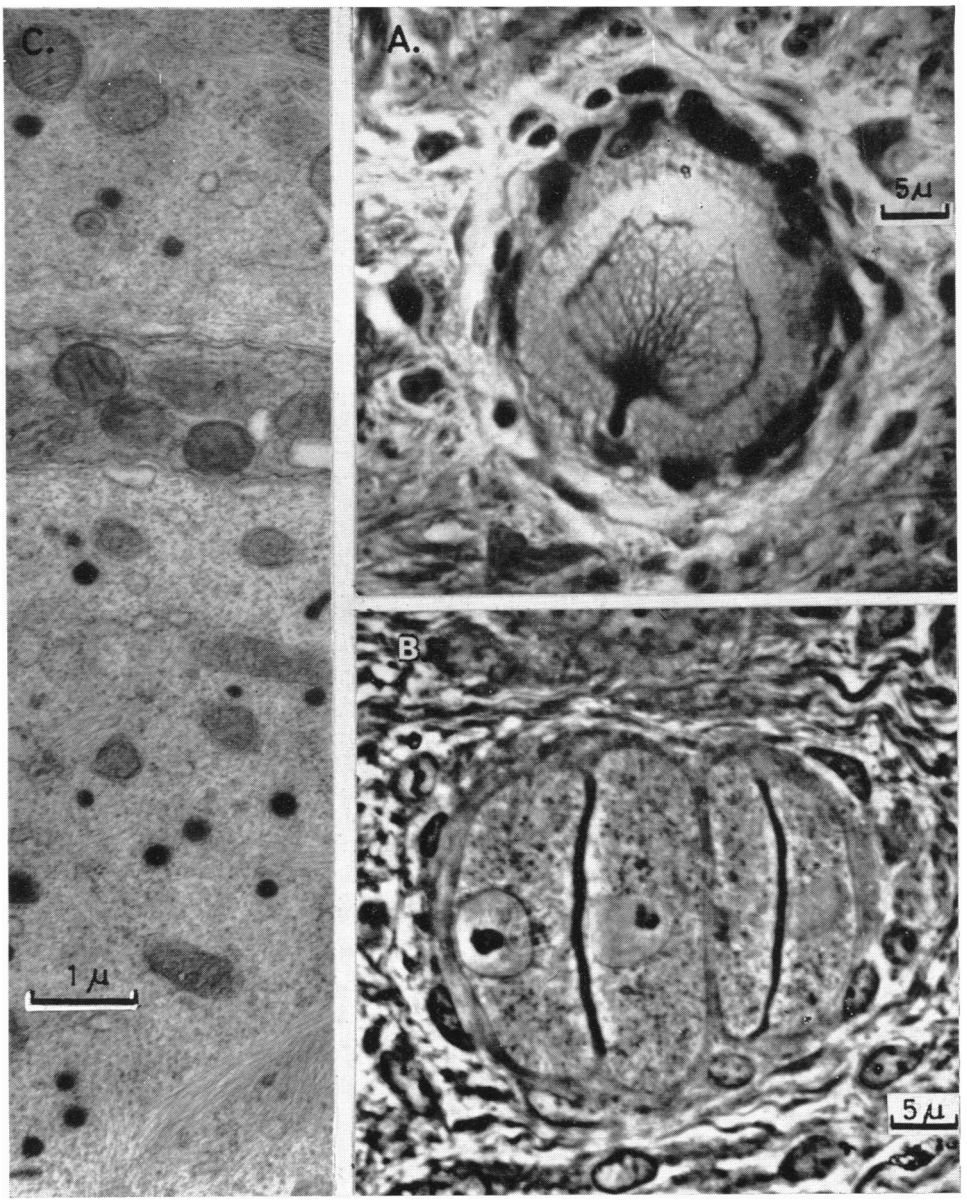

Fig. 1

The majority of the bags become electron-dense and granular with 'darkened' mitochondria. The surface of the bag becomes distorted showing thin processes wedged in between the adjacent profiles. Glycogen-rich glial processes engulf or displace the degene-

rating bag (Fig. 2a) but only infrequently surround completely the post-synaptic process (i.e. spine tips). Phagocytosis, apparently by astrocytes, is advanced after 48 h and contacts on both spine tips and dendritic shafts are involved.

By 3–7 d, some post-synaptic processes lose their pre-synaptic bag and the thickenings are now contacted by glia (Fig. 2b). Other post-synaptic processes, however, continue to maintain contact with degenerating bags which have not been removed by the glia. Longer survival times show degenerative debris in decreasing amounts but 12 weeks after the lesion remnants of degenerating bags remain in contact with dendritic spines. Possibly those post-synaptic processes which lose their degenerated pre-synaptic bags in the early stages may become re-innervated by adjacent or new synaptic bags.

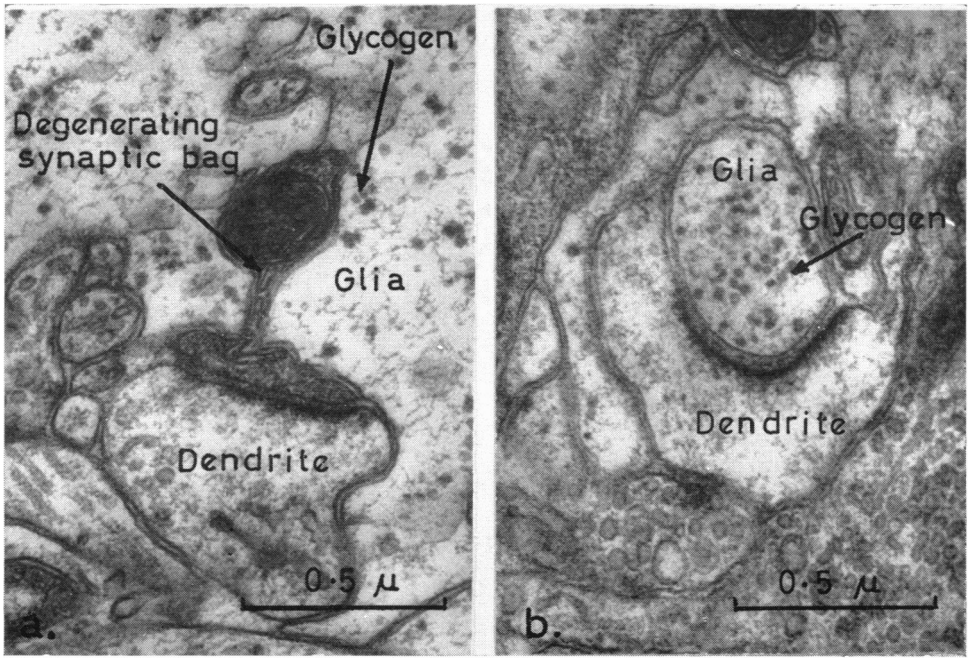

Fig. 2

The morphological polarization of kinocilia in the *Octopus* statocyst.
By V. C. Barber. *University College London* (Figs. 3, 4)

Both the macula and crista are composed of hair cells and supporting cells, and below them is a nerve plexus with a third type of cell and several sorts of synapses (Barber, *J. Microscop.* **4**, 1965; *Z. Zellforsch.* **70**, 1966). The hair and supporting cells bear microvilli at their distal ends. The kinocilia borne by each hair cell have the typical 9 + 2 arrangement of filaments and are arranged in elongated groups of up to 200. Each group is approximately parallel to adjacent groups. Transverse section of part of a group from the macula, (Fig. 3) shows that the two central fibres of each cilium are orientated in line with the long axis of the group (arrow shows axis). Each kinocilium has a club-shaped basal foot attached to its basal body. A slightly oblique transverse section of the distal end of a macula hair cell (Fig. 4) shows that these feet (arrows) are parallel to each other and are at right angles to the line of the central fibres of their cilia and to the long axis of the group. The direction of movement of the cilia is at right angles to this long axis so each cilium has a polarity with regard to the direction of movement that it detects. A similar orientation of the kinocilia has been shown in some vertebrate vestibular systems where such cells are

undirectional in response (Flock & Duvall, *J. Cell Biol.* **25**, 1965). These cells in the crista of *Octopus* also show an undirectional response to angular acceleration (Maturana & Sperling, *Nature, Lond.*, **197**, 1963).

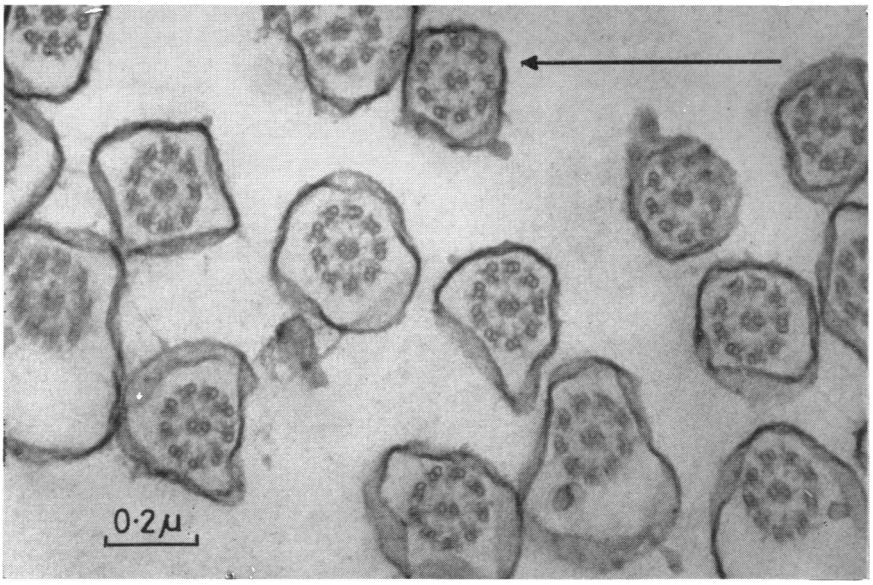

Fig. 3

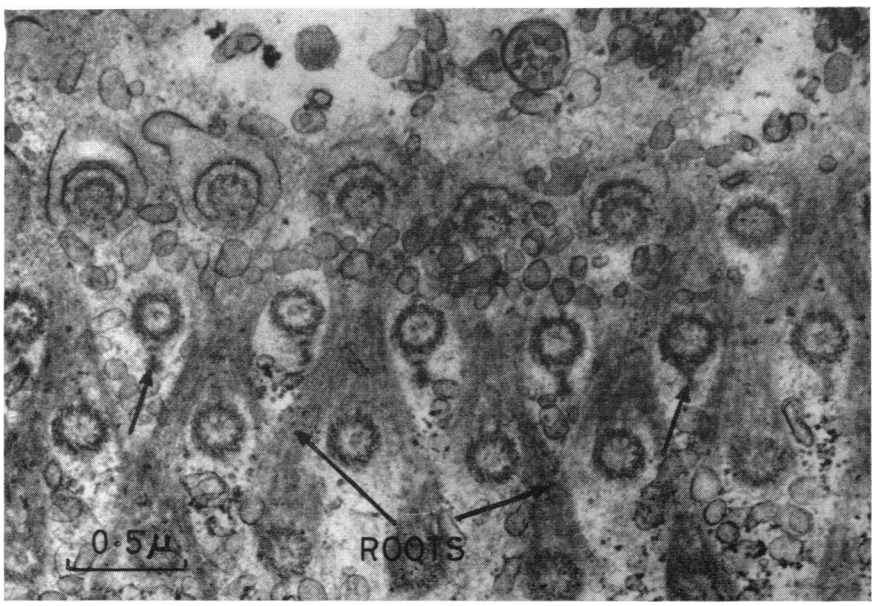

Fig. 4

Tangential patterns of dendrites and axons in three auditory areas of the cat's cerebral cortex. By W. C. Wong. *University College, London*

Colonnier (*J. Anat., Lond.*, **98**, 1964) showed that in a tangential plane the dendritic fields of many stellate neurons in the visual cortex were oval in shape. In the present work further aspects of the tangential organization have been investigated in three auditory areas (AI, Ep and association, after Woolsey) of the cats' cerebral cortex, stained by Golgi Kopsch after glutaraldehyde or formol fixation. The fields of basal dendrites and of terminal apical bushes of pyramidal neurons, and the dendritic fields of stellate neurons were again measured. The shape of dendritic fields varied greatly from the completely circular field to those showing extreme 'polarity'. Circular basal dendritic fields were common in AI and predominated in Ep and the association area. In all areas oval basal dendritic fields were rare. In contrast, among stellate neurons in all areas oval and circular fields occurred with approximately equal frequency.

In Holmes preparations the orientation of the tangential fibres was measured in terms of four 45° angles using as a 0° baseline the long axis of each gyrus. In AI the overall direction of the fibres appeared random. In Ep oblique fibres predominated and in the association area horizontal fibres (in the direction of the long axis of the middle suprasylvian gyrus) predominated from layers III to VI.

The ratio of 1:1 (in the visual cortex it is 3:1) oval to circular stellate fields, the absence of a preferential orientation among the oval dendritic fields and the lack of a consistent pattern of orientation of the tangential fibres in Holmes preparations are different from the spatial patterns described in the visual cortex.

Aldehyde fixation of nerve fibres. By James E. Vaughn and Alan Peters. *United Cerebral Palsy Foundation and University of Edinburgh*

A standard for fixation of nervous tissue has been established in material prepared by perfusion with osmic acid. The advantage of fixation by perfusion rather than immersion is that tissue can be well preserved *in situ* so that the distortion produced by the removal of fresh tissue is avoided. This makes it possible to investigate deep structures that are not readily accessible to fixation by immersion.

However, perfusion with osmium has certain disadvantages which have stimulated the recent use of aldehydes, the most useful of which are formaldehyde and glutaraldehyde. Glutaraldehyde preserves more cytoplasmic background material than osmium, but unfortunately causes an overall fuzziness that detracts from the quality of electron microscopic images. This fuzziness may be due to a polymerization of glutaraldehyde in the tissue. Formaldehyde, prepared from paraformaldehyde, produces distinct images but is not as effective as either osmium or glutaraldehyde in preserving cytoplasmic detail. Microtubules, for example, are not well fixed, and many myelin sheaths undergo a type of lamellar splitting.

Since perfusion either with glutaraldehyde or formaldehyde alone does not produce fixation that is as good as osmium, they have been mixed together in an attempt to both negate the undesirable effects of each aldehyde while retaining their virtues. A successful combination for fixing nerve fibres by perfusion is a solution containing 0·5 % glutaraldehyde and 4 % formaldehyde in Millonig's phosphate buffer at pH 7·4. The fixation produced by this mixture is comparable to that in osmium perfused preparations. The lack of clarity produced by glutaraldehyde alone is absent while, even at this low concentration, its virtues in fixing cytoplasmic constituents are still retained.

A short fluorescence technique for the demonstration of adrenergic nerves. By T. L. B. Spriggs, J. D. Lever, P. M. Rees and J. D. P. Graham. *University College, Cardiff*

Cryostat sections (18 μm thick) of rat and cat pancreas and cat nictitating membrane were thawed on to glass slides and subsequently dried over P_2O_5 for $1\frac{1}{2}$ h in a closed desiccator. Specimens were then transferred into a second desiccator containing paraformaldehyde powder. The vessel was closed and placed in an oven at 80 °C for 1 h. Falck & Owman (*Acta Univ. Lund*, **11**, 1965) have shown that identical samples of paraformaldehyde absorb different amounts of moisture depending upon the relative humidity at which they are stored (for 1 week). On subsequent heating these samples release both formaldehyde gas and specific quantities of water vapour.

The water content of paraformaldehyde necessary to procure optimal fluorescence varies according to the tissue and occasionally for the same tissue between animals. The routine use of 3 gassing desiccators respectively containing paraformaldehyde previously stored at 80·5, 85 or 88·8 % humidities usually ensures that at least one set of specimens will display optimal fluorescence.

After gassing, specimens were glycerine-mounted before examination with a fluorescence microscope. The entire procedure from removing the tissue from the animal to observing fluorescence in the microscope, is accomplished in a single working day.

The paravascular axons in rat and cat pancreas were visualized as a beaded lemon-yellow fluorescent network, but not in animals previously reserpinized. Smooth muscle of the cat nictitating membrane was seen to be profusely supplied with nerves exhibiting a similar beaded fluorescence which was not visualized in animals after superior cervical ganglionectomy.

Cytological changes within β cells of the rabbit pancreas stimulated *in vitro*. A quantitave study. By J. A. Findley* J. R. Gill† G. Irvine,* J. C. Lever* and P. J. Randle†, *University College, Cardiff* and University of Bristol†.

Small pieces of rabbit pancreas were maintained *in vitro* in an enriched bicarbonate buffer as described by Coore & Randle (*Biochem. J.* **93**, 1964). Pancreatic specimens were obtained before incubation and after 30, 40, and 60 min incubation in this basic medium (glucose 60 mg %). At 30 min some of the specimens were transferred to medium containing (1) glucose 300 mg % or (2) tolbutamide 20 mg %, glucose 60 mg %: samples were then taken after 10 and 30 min stimulation. Specimens were osmic-fixed and araldite-embedded for electron microscopy. Clear cytological definition indicated cell survival during the period of the experiment. Characteristic secretory granules individually enclosed by a smooth membranous sac were observed in the β cells. In electron micrographs of all specimens some of these sacs showed a single perforation.

The following quantitative observations were made from electron micrographs of unstimulated material (from the basic medium) and stimulated material: (1) number of secretory granules/unit area of β cell cytoplasm (2) percentage of sacs showing perforation; (3) number of sac contacts/unit length of plasma membrane. The values obtained from stimulated material were compared with the values from material incubated for 30 min in the basic medium.

The secretory granule population of β cell cytoplasm did not differ significantly between any of the specimens. In tolbutamide-treated specimens (1) there was a probably significant reduction in the percentage of perforated sacs after 10 min stimulation, while at 30 min there was a highly significant increase; (2) sac contacts with the plasma membrane were increased in the 10 min specimens only. In the glucose-stimulated gland (1) there was a probably significant increase in the percentage of perforated sacs in 10 min specimens only; (2) there was no significant change in the number of sac contacts with the plasma membrane.

Cytomorphology of milk secretion in the rat. By G. K. Benson and Barbara Brown. *New York State Veterinary College and University of Liverpool*

Observations were made on mammary tissue taken from lactating rats at intervals of from 2 to 24 h after separating the mother from her pups. The rats were in their 10th to 13th day of lactation.

Two types of secretory vacuoles can be seen by electron microscopy, namely small vacuoles containing dark granules, probably protein, and larger vacuoles containing fat. The two types of vacuole are present at various levels in the cytoplasm and at the cell surface adjacent to the alveolar lumen, where they rupture, releasing their contents.

The large fat droplets appear to be released intact but within the alveolar lumen there is some evidence of their breakdown into smaller droplets. Sometimes several fat droplets appear to coalesce in the cytoplasm prior to rupture.

In mammary tissues removed at intervals of up to 10 h after separating mothers from pups, no cytoplasm appears to be lost in the secretory process, the cell membranes apparently being sealed by the vacuolar membranes. However, in tissues taken later than 10 h after removal of the pups there is evidence in some cells of widespread breakdown of the cell membrane with consequent release of fat, protein and cytoplasmic constituents into the alveolar lumen. In these circumstances the large fat droplets are sometimes surrounded by a ring of cytoplasm and cytoplasmic organelles.

These findings, while confirming that secretion of milk by the alveolar cells may occur without the loss of cytoplasmic components as reported by other workers, indicate that prolonged secretion without milk removal may cause cell breakdown.

This investigation was supported by U.S. Public Health Service Grant FR 05462–02 to N.Y.S. Veterinary College.

The proteinpolysaccharide of cartilage and its relationship to collagen. By J. W. Smith, A. Serafini-Fracasini and T. Peters. *University of St Andrews*

By staining with bismuth nitrate at pH 1·2 proteinpolysaccharide has been visualized in the electron microscope in intact bovine nasal cartilage and articular cartilage and in aqueous extracts of the former tissue. In the aqueous extracts, the macromolecules of proteinpolysaccharide are evident as linear aggregates of particles having a particle weight of about 56000. In the tissues, a proportion of these macromolecules are attached to collagen, being wound transversely round the fibre over the a and b_1 bands of each 640A period.

Carbon replica study of ameloblast-enamel interface. By A. Boyde. *The London Hospital Medical College*

The morphology of the surface resulting when the enamel-organ is stripped from developing enamel has been studied by direct, one-stage carbon replication. That the plane of cleavage was between the Tomes processes of the ameloblasts and the surface of their secretory product was verified by studying ultra-thin sections cut normal to the surface of the stripped enamel. Better stripping resulted when the tooth-germs had been previously fixed in neutral formol saline. Surfaces were held at 45° to the carbon arc and rotated whilst the carbon was evaporated. The tooth was then digested away from the carbon. Stereo-pair electron-micrographs of the unshadowed carbon replica show more than adequate contrast when viewed stereoscopically. Photogrammetric measurements and contour maps were made using a Hilger and Watts 'Stereometer' and Plasticine models using a Hilger and Watts 'Stereosketch'. The results obtained by these methods confirm the nature of the surface of developing enamel deduced from previous studies using ultra-thin sections for the EM, scanning electron microscopy and wax reconstructions. The presence of a complete, circumferential, cliff-like wall surrounding each Pattern 1 type depression is confirmed. The rows of future 'inter-row sheet' material in Pattern 2 enamels

are quite prominent, i.e. they form in advance of the bridges of material between depressions (ameloblasts) in the same row. The future 'winged process' regions of Pattern 3 prisms are prominent from the developing surface to the degree that they are noticeable in the fully formed enamel. Findings include the nature of the two-stage filling-in process responsible for the formation of 'prisms within prisms' and the developmental mechanism by which Pattern 3 'prism sheaths' are connected to form arcades.

Electron stereoscopy of tissue sections. By Robin Willis and E. G. Gray. *University College, London*

The depth of focus (0·1 μm) of a light microscope is less than the resolution (0·2 μm). On the other hand the depth of focus of the EM (0·2 μm) is 200 × more than the resolution (10 Å) and nearly 4 × more than the section thickness (600 Å). This means that organelles with dimensions below 600 Å, e.g. ribosomes, neurofilaments, synaptic vesicles, membrane profiles, etc., lie enclosed within the thickness of the section and so are viewed with the EM not as sections but as whole structures. Thus more complete information can be gained by tilting the organelle within the section in the electron beam to show its various aspects, and with suitable tilt angles, pairs of micrographs can be viewed stereoscopically.

We have examined various tissues using a 'Valdré' cartridge to obtain tilts up to 45°, and find that angles up to and exceeding 20° are suitable for stereoscopy. Due to the rotation of the electron beam it is necessary to orientate the micrographs to obtain maximum stereo-depth. The angle of orientation is determined by plotting the angular rotation observed on the fluorescent screen against magnification.

Electron stereoscopy is, of course, not new, yet in spite of its theoretical advantages it has gained surprisingly little popularity in the examination of plastic sections of biological material. We suspect that this is because a psychological factor is involved for we find that while simple organelles appear in depth in a stereo-pair of micrographs, more complex structures in the same micrographs that are not understood at the outset appear flat. Various examples of stereoscopy were presented to illustrate the above remarks.

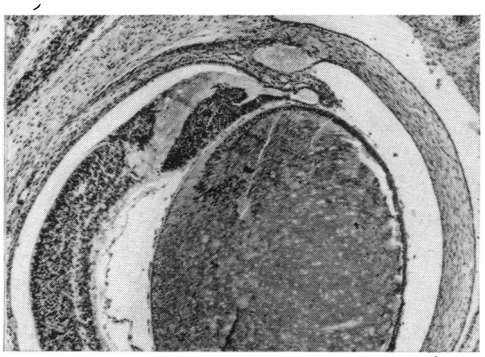

Fig. 5

Fig. 6

Abnormal migrations of optic and olfactory fibres, and deductions therefrom. By A. Giroud. *Faculté de Médecine, Paris* (Figs 5, 6)

In the normal embryonic eye the optic fibres migrate towards the brain by way of the optic peduncle and form the optic nerve. In many abnormal eyes of rats and mice (induced by drugs, or infections such as toxoplasmosis), the optic fibres may run in opposite directions and get to the iris and the cornea (Fig. 5), consequently the optic nerve is lacking or

remains very small. Even in one case of cyclopian eye, the optic fibres have been seen running towards the nasal cavities.

In the normal embryo the olfactory fibres run towards the telencephalon and consequently an olfactory bulb develops. In cyclocephalic embryos (rats and mice) the olfactory fibres do not get to the telencephalon and the olfactory bulb is lacking. The olfactory fibres cross the lamina cribrosa, but remain separated from the brain; however, they continue to grow and mitosis of their glial cells results in the formation of a mass of intermingled fibres. The same fact may be observed in arrhinencephalic human foetuses. From this mass, some fascicles of olfactory fibres migrate away from the brain, some run through the skull towards the skin, while some others run over the nasal cavities (Fig. 6).

In many cases the optic and olfactory nerves may migrate in a direction opposite to the normal one. It is difficult to explain such migration by some predetermined path. The old explanation of Cajal may be the best. Some attraction or some repulsion (perhaps of a chemical nature) may explain the abnormal as well as the normal migration of nerves.

The filiform papillae of the rat tongue: their structure and histochemistry. By A. K. CANE and R. I. C. SPEARMAN. *University College Hospital Medical School*

We have found that the rat tongue epidermis undergoes several diverse forms of keratinization in its various regions. This contrasts with the body and tail skin which forms relatively few different types of horny structures.

The filiform papillae are discrete epidermal horny appendages with their own germinal centres. Each papilla has three distinct parts. The anterior convex side has a horny layer composed of solid keratinized cells without basophilic nuclei and is formed over a modified granular layer. The posterior concave side develops a thin solid horny layer without any underlying granular layer. A horny spine rich in keratin disulphide bonds is found in the centre of the papilla. The spine cells appear to be shed in a characteristic manner from the tip of the spine.

The dorsal interpapillary epidermis has a 'granular layer' containing large globular cytoplasmic bodies and a layer of solid horny cells is formed. Here, however, unlike in the filiform papillae, disulphide bonds are more concentrated around the cell membranes. A different type of horny layer is found ventrally in the tongue.

The distribution of cystine disulphide bonds, bound sulphydryl groups, bound phospholipids, and bound calcium differs in each region and is related to the different types of keratinization occurring. There are also enzyme differences.

The filiform papillae of the cat, guinea-pig, rat, mouse and rabbit vary appreciably in structure and composition.

Some features of prosimian pituitary glands.
By R. L. HOLMES. *University of Leeds* (Fig. 7)

Pituitary glands of several prosimii (*Galago crassicaudatus*, *Perodictitus potto* and the slender loris) have a number of features in common. Thus, many cells of the pars distalis of each of these species are arranged in follicles, made up entirely of either chromophobes or chromophils, or of a mixture of cells. The follicles usually contain a globule of PAS-positive colloid, as in the potto (Fig. 7 A). Rosettes of cells with no central lumen also occur, as well as colloid droplets outside follicles, as in the galago (Fig. 7 B). The pars distalis of another galago, *G. demidovii* shows few follicles except superiorly.

In each of these four species mucoid cells predominate in the centro-rostral zone of the pars distalis, and acidophils caudo-laterally, although there are no *extensive* zones of *single* cell types. Grouping together of cells having similar staining characteristics is common (e.g. mucoid cells in Fig. 7B).

The pars intermedia in the first three species listed is thick and contains colloid-filled follicles, but in *G. demidovii* it is less conspicuous. The pars tuberalis in all four consists of prominent cellular follicles containing colloid, surrounded by vascular connective tissue.

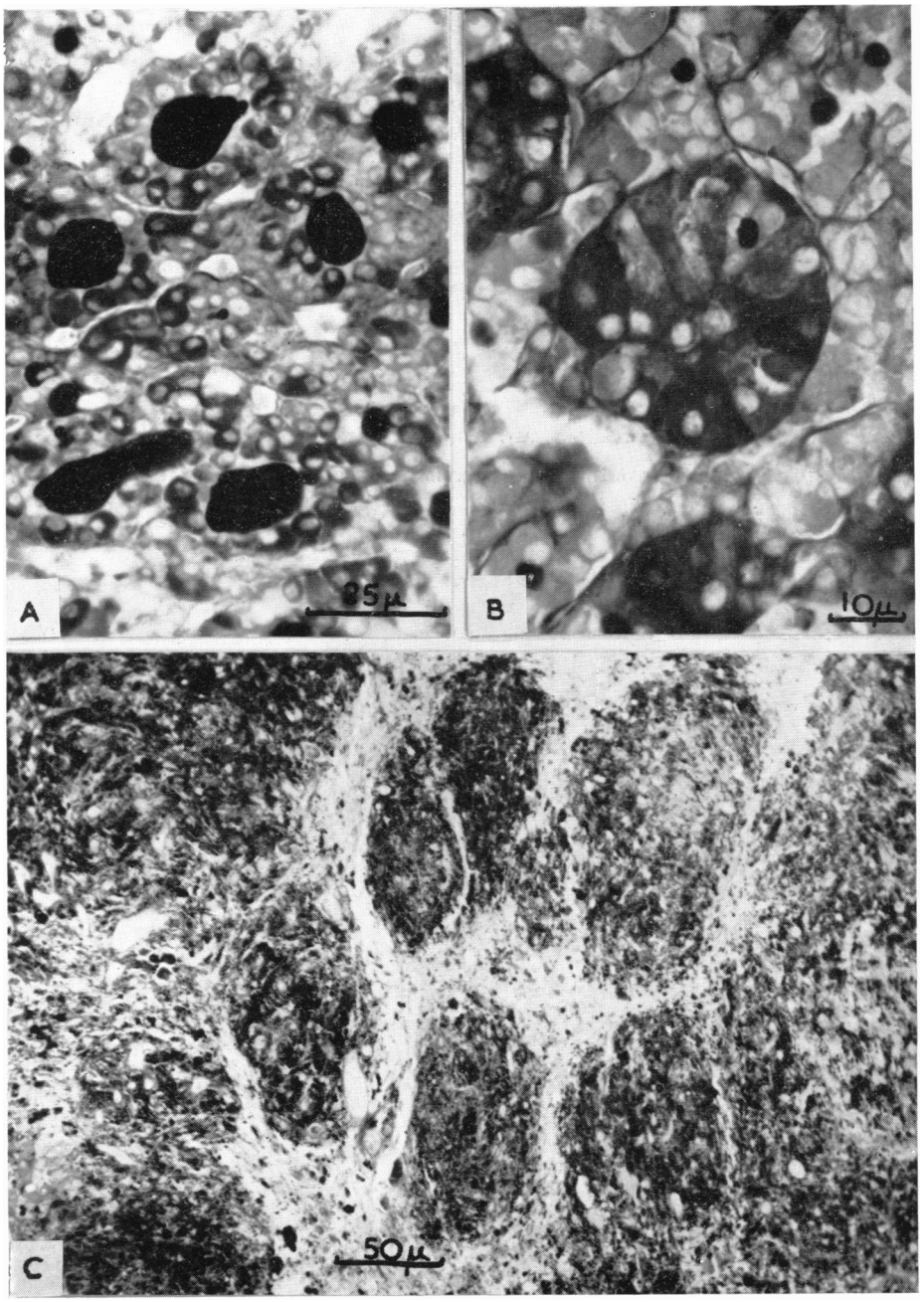

Fig. 7

The neural process of the potto (Fig. 7 C), and to a lesser extent that of *G. crassicaudatus*, shows striking lobules of Alcian-blue positive neurosecretory fibres, separated by paler-staining tissue. Dendritic-type pigment cells occur in the capsules and between groups

of cells in the partes distalis and intermedia in the potto and *G. crassicaudatus*. These also occur around neurohypophysial blood vessels in the latter species.

Follicles in the pars distalis are a feature of immature, or sometimes of primitive pituitaries. The pattern described here might suggest either retention of embryonic characteristics, or a secondary specialization, and perhaps that the colloid may be of functional significance. A lobular neurohypophysial pattern is unusual in mammals.

Cholinesterase and sodium transport in the supra-orbital gland of the duck. By JULIA FOURMAN. *University of Leeds*

The supra-orbital gland of the domestic duck secretes sodium chloride when the plasma sodium concentration is high. We have demonstrated cholinesterase activity in the secretory cells of this gland and and by the use of selective inhibitors shown that the enzyme is butyrylcholinesterase.

The activity of this enzyme in the glandular cells has been studied in the supra-orbital glands from twelve ducks. Six of these had previously been given sodium chloride (1 g NaCl in 20 ml of water at two hourly intervals, for 6 h before the gland was removed); the other six served as controls.

The glands of the control animals did not produce any visible secretion and showed slight cholinesterase activity. The glands of the animals given salt, secreted large amounts of fluid which contained 592–720 m-equiv/l. of sodium, and the secretory cells gave an intense reaction for cholinesterase.

Thus it appears that cholinesterase activity of the sodium secreting cells is increased when sodium transport is increased, a finding which is in keeping with observations on other tissues. These results suggest that butyrylcholinesterase activity may in some cells be related to sodium transport, a hypothesis which is suggested by the presence of an enzyme hydrolysing the same choline ester at the site of maximum transport in the renal tubule.

Trypan blue and the homograft reaction. By K. BAXBY and R. J. SCOTHORNE. *University of Newcastle upon Tyne*

There have been several claims that trypan blue, administered to the host animal, prolongs the survival of tumour transplants and of homografts of normal tissue; it is sometimes assumed that trypan blue acts by 'blockade' of the macrophage system. In the present study rabbits received skin homografts on one ear (method of Scothorne & McGregor, 1955) and one of the following treatments:

(1) Intravenous trypan blue (B.D.H. 'for vital staining', 1% solution. Dosage: 20 mg/kg or 30 mg/kg 4 days before grafting and daily thereafter until the time of graft breakdown). Controls received intravenous normal saline. Mean survival times: control group (12 rabbits) $6{\cdot}9 \pm 1{\cdot}2$ days; experimental group (12 rabbits) $11{\cdot}9 \pm 2{\cdot}6$ days (highly significant prolongation of survival: $P < 0{\cdot}001$).

(2) Intraperitoneal trypan blue, in a single dose of 137 mg/kg 3 days before grafting. Survival of skin homografts was not significantly extended contrary to the findings of Brent & Medawar (*Proc. Roy. Soc.* **B. 155,** 1962) using similar dosages in mice.

(3) In order to produce a maximal 'blockade' of macrophages in the first regional node draining the graft, rabbits were injected intradermally (in the ear which was to receive the graft) with 0·1 ml of a carbon suspension (Pelikan C11/143a, 1 : 2 in distilled water) on each of 4 successive days, beginning 2 days before grafting. Mean survival: controls (12 animals) $6{\cdot}9 \pm 1{\cdot}2$ days; experimental group (18 animals) $8{\cdot}9 \pm 1{\cdot}2$ days (no significant prolongation of survival).

It is concluded (1) that trypan blue, administered intravenously in high dosage, does prolong skin homograft survival in rabbits; (2) that, almost certainly, trypan blue does not act by 'blockade' of the macrophage system; maximal 'blockade' of macrophages in the first regional node by carbon does not prolong homograft survival.

Preliminary studies on the lymphatic drainage of the guinea-pig thymus with special reference to the extrinsic vessels. By P. F. HARRIS and W. R. TEMPLETON. *University of Sheffield* (Figs 8, 9)

In rodents the thymus is considered to produce many lymphocytes, but most are thought to remain *in situ*. At least two possible emigration routes exist. Recent workers have concentrated on venous channels and have considered lymphatics to be unimportant (Ernstrom *et al.*, *Nature, London.*, **207**, 1965). Although intra- and inter-lobular vessels are well-documented, there is little reference to extrinsic lymphatics and their significance in transporting lymphocytes from the thymus.

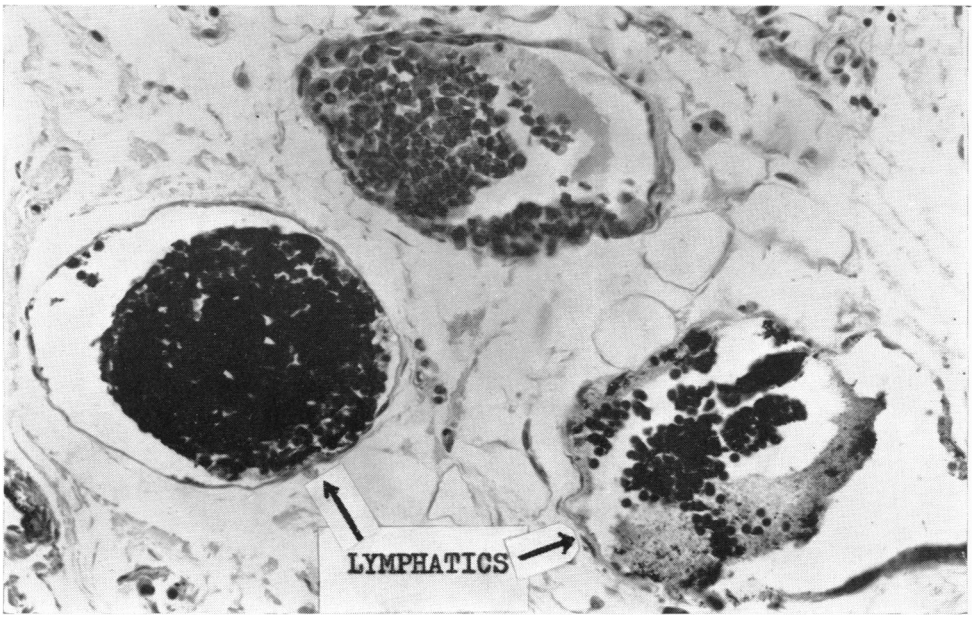

Fig. 8

Thymic lymphatics in young guinea-pigs were studied macro- and microscopically by direct injection into the organ of the supernatant from a carbon suspension (C11/1431a, Wagner), centrifuged at 5000 r.p.m. for 15 min, 1 vol. of which was mixed with 99 vol. of a 1 % isotonic solution of Pontamine Sky Blue 6 BX (Gurr). The main cervical lymphatics were outlined by injecting the mixture into the tongue and external ear.

No afferent vessels were found. A juxta-medullary plexus draining via inter-lobular lymphatics to the surface of the thymus was confirmed. Large efferent lymphatics accompany three main vascular bundles from the thymus. These contained carbon and numerous thymic lymphocytes (Fig. 8). They are: (*a*) superior pole vessels draining into the deep cervical duct, (*b*) medial vessels joining lymphatics accompanying the anterior jugular (inter-thymic) vein, and (*c*) lateral vessels draining into a lateral cervical trunk. All eventually empty into a constant cervical lymph-hode lying postero-inferior to the lower pole of each lobe. A separate efferent lymphatic also enters this node from the lower deep aspect of the thymus. Thus, an injection of carbon into the thymus becomes localized in the node (Fig. 9) and from this a main duct drains into the jugular vein at the root of the neck. Preliminary experiments using various methods of labelling thymic lymphocytes are being performed.

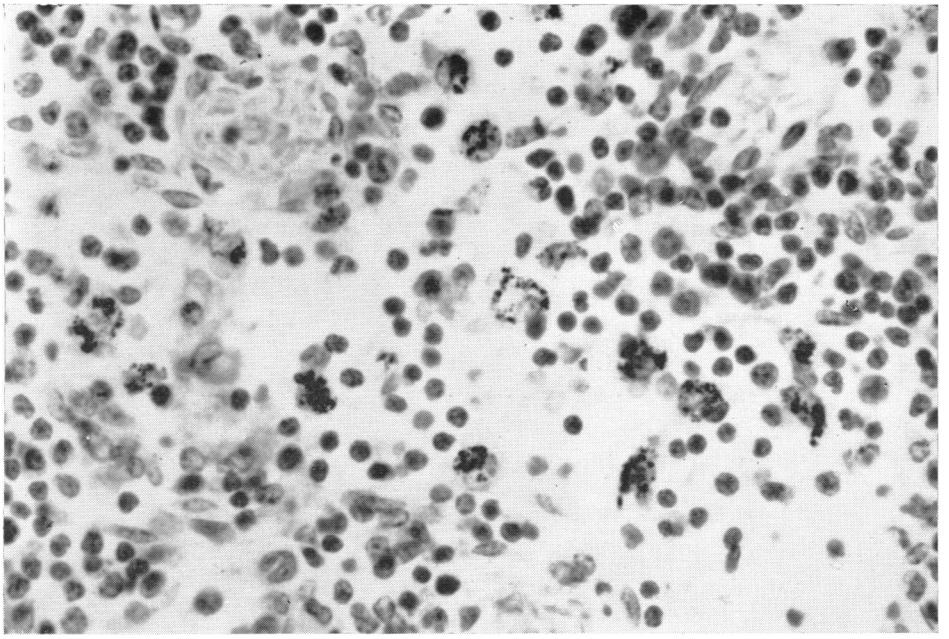

Fig. 9

The structure of stimulated peritoneal macrophages.
By Ian Carr. *University of Sheffield*

Stimulated macrophages have been obtained by injecting 0·1 ml of Hanks's solution, with and without 10 mg glyceryl trioleate into the peritoneal cavity of male white mice. Cells were harvested by washing out in Hanks's solution at varying periods up to 10 days. These cells, stimulated *in vivo*, were compared with control cells obtained merely by washing out the peritoneal cavity, and with cells stimulated *in vitro*. The cells were examined histochemically and by electron microscopy.

The cells stimulated *in vivo* varied more in size and shape than the controls, and were on average larger. The cells contained more acid phosphatase and non-specific esterase, as demonstrated histochemically, and had longer and more prominent processes.

These findings are in keeping with the hypothesis that two of the main occurrences in stimulation of the reticulo-endothelial system are an increase in the surface motility of macrophages, and an increase in synthesis of hydrolytic enzymes.

The effect of whole body gamma radiation on subsequent phytohaemagglutinin culture of rat blood. By W. K. Metcalf. *University of Bristol*

The suggestion that the heterogeneous blood lymphocyte population may include the 'haemopoietic stem cell' has been supported by the occurrence of marrow lymphocytosis preceding erythropoiesis and granulopoiesis following sublethal gamma radiation, and by the production of blast-like cells, capable of mitosis, from small lymphocytes in phytohaemagglutinin (PHA) cultures. To test the relevance of these observations, whole body gamma radiation in the dose range 120–600 R has been administered to adult Lister hooded rats followed by serial 72 h PHA blood culture.

With this dose, there is an immediate (less than 15 h) fivefold decrease in the yield of

leucocytes for culture produced by our standard technique, and virtually no living cells were found in such cultures after 72 h incubation. However, within a week of the radiation, depending on the dose, large macrophage-like cells capable of mitosis began to be found in increasing numbers in the cultures. With doses of 120 and 200R, typical 'PHA' cells again began to be found in the cultures 3 and 5 weeks after radiation respectively. With larger doses, we have not yet been able to produce typical 'PHA' cells in subsequent culture even after long intervals (up to 90 days) when the animals appear to have otherwise completely recovered.

These experiments suggest that, if the blood lymphocytes do include the stem cell, those that produce 'macrophages' in culture are more likely candidates than those which respond to PHA. It is interesting to note that bone marrow, transfusion of which can confer protection against a previous lethal dose of radiation, appears to contain only the latter type of lymphocyte.

Increased vascular permeability in the reproductive organs of cadmium chloride-treated male rats. By E. J. Glegg and Ian Carr. *University of Sheffield.* (Fig. 10)

Several investigations have suggested that vascular changes may be responsible for the severe testicular damage produced by small doses of cadmium salts and recently, Waites

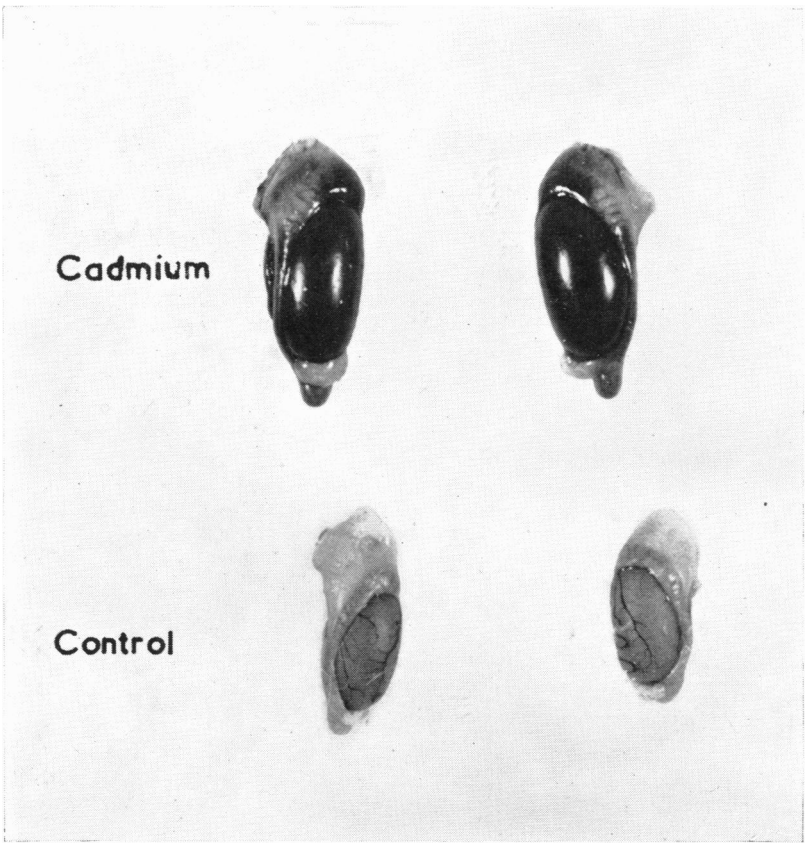

Fig. 10

& Setchell (*J. Endocrin.*, in press) have demonstrated increased vascular permeability in the testis and epididymis after cadmium, using ^{131}I iodo-antipyrine as a marker.

In the present investigation adult male rats received, either intraperitoneally or subcutaneously, cadmium chloride (0·5 mg/100 g body weight); control animals received equivalent volumes of Ringer's solution. As an indicator of increased vascular permeability Evans' blue (6 mg/100 g body weight) was given intravenously 1 h before sacrifice. The animals were killed between 100 min and 24 h after the administration of cadmium.

Cadmium-treated animals showed a variable and transient blueing of the testes during the first half hour. At 1½ h there was again slight blueing, but at 2 h the testis and initial segment of the epididymis were very blue; the findings were indentical in all animals during the remainder of the 24 h. Additionally, at 6 and 12 h the whole of the epididymis except the isthmus was blue, as was the proximal ductus deferens. Figure 10 shows the difference in appearance of the testes of experimental and control animals at 6 h.

Most of the animals also received saccharated ferric oxide solution intravenously at the same time as the Evans blue. Histological examination after Prussian blue staining confirmed that vascular permeability in the testis and epididymis was increased and also suggested the possibility of vascular stasis in these organs.

Comparison of histochemical methods for β-glucuronidase in rat ovary and placenta. By D. Bulmer. *University of Manchester*

The histochemical distribution of β-glucuronidase has been studied in rat ovary and placenta with 1-naphthyl glucuronide, 8-hydroxyquinoline glucuronide and naphthol AS-BI glucuronide as substrates. The naphthyl glucuronide simultaneous coupling method gives satisfactory results with fast blue BB as diazonium salt, strong activity is demonstrated in metrial gland cells after 30 min incubation, and even with 2 h incubation background staining is minimal. A simultaneous coupling procedure with 8-hydroxyquinoline glucuronide is less satisfactory. Using fast dark blue R as diazonium salt intense staining occurs after a short incubation, but there is marked non-specific background coloration. With fast blue BB or fast red violet LB the final reaction product is an orange-red colour, distinct from the yellowish background stain, but incubation periods of 1–2 h are necessary. The lack of colour contrast between reaction product and background stain makes identification of weakly reactive sites difficult. With the naphthol AS-BI glucuronide post-coupling method (Fishman & Goldman, *J. Histochem. Cytochem.* **13**, 1965) a precise finely granular localization is obtained.

All three substrates show a similar distribution of β-glucuronidase activity. In the placenta the most pronounced reaction is in metrial gland cells, and with naphthol AS-BI glucuronide this is clearly localized on the glycoprotein granules. Activity is also demonstrated in decidua, visceral endoderm of the yolk sac, and labyrinthine trophoblast. In the ovary macrophages, atretic follicles, theca interna and interstitial cells show strong or moderate activity, while in corpora lutea the reaction increases with ageing and degeneration. Comparison with the distribution of other hydrolytic enzymes suggests that the methods employed demonstrate a lysosomal β-glucuronidase, and the results differ markedly from those reported previously for the Fishman-Baker ferric hydroxyquinoline technique.

Fine structure of the nucleus in the primordial oocyte of primates. By T. G. Baker and L. L. Franchi. *University of Birmingham* (Fig. 11)

Foetal, neonatal and pre-pubertal human and monkey ovaries were fixed in glutaraldehyde and/or osmium tetroxide, embedded in Vestopal and examined with the electron microscope. Oogonia and oocytes at the leptotene to the diplotene stages of meiotic prophase were identified by comparison with light microscopical preparations.

The chromosomal threads seen in oocytes at the leptotene (A, Fig. 11), zygotene and pachytene (B, Fig. 11) stages are essentially similar in appearance to those in corresponding

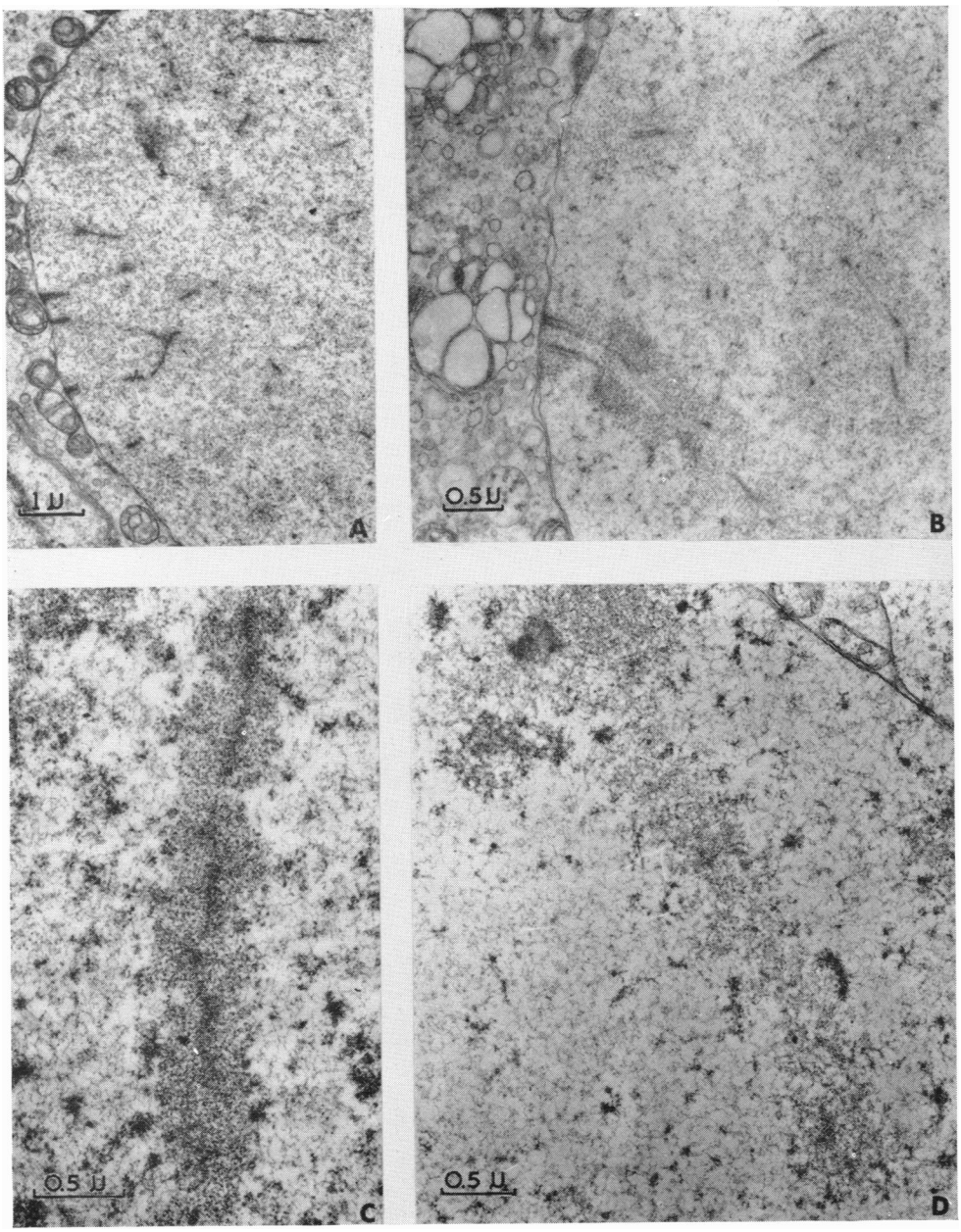

Fig. 11

cells in the rat (Franchi & Mandl, *Proc. R. Soc.* B. **157**, 1962). In contrast to the primordial oocytes in the rat, those in primates contain well-defined threads, which have been shown to be in the diplotene configuration. The chromosomal threads in primate oocytes also possess an investing sheath of electron-dense material which is most highly organized at

pachytene (B, Fig. 11) and diplotene (C, Fig. 11). In the primordial oocyte this material frequently forms symmetrically arranged lateral projections, composed of coiled fibrils, which are apparently reflected back on to the axis to form loops (D, Fig. 11). This structure is similar to that of the lampbrush chromosomes in oocytes of lower vertebrates.

It has been suggested that variations in the radiation-reponse of germ cells may be due to differences in chromosomal structure. The present observations may therefore help to explain the marked difference in radiosensitivity of primordial oocytes in primates and rodents.

Dermatoglyphic studies in a mentally defective population.
By M. N. RASHAD. *University of Edinburgh*

5372 mental defectives in seventeen institutions were examined (2852 males, 2520 females). Assessment of finger ridge pattern was carried out. Data from Scotland Yard for 5000 individuals was used as controls (64 % ulnar loops, 25·4 % whorls, 4·9 % arches and 5·7 % radial loops).

Of the 2852 males examined, 259 were mongols and twenty cases had evidence of sex-chromosome abnormalities (nine cases *XXY*, five cases *XXXY*, four cases *XXYY*, one case *XXXXY* and one case *XXY*/trisomy 21). Mongols showed less variation than controls. There were fewer whorls (10·9 %), fewer arches (2·4 %) and an increase in ulnar loops (85·4 %). Cases with abnormal sex chromosomes showed an increase in arches (19·5 %) and a corresponding decrease in ulnar loops (54 %). Other defectives had 59·9 % ulnar loops, 28·2 % whorls, 7·9 % arches and 4·3 % radial loops.

Of the 2520 females examined, 212 were mongols and eight cases had evidence of abnormal sex chromosomes (six cases *XXX*, one case *XO*/*XXX* and one case *XXXX*). Female mongols showed similar features to male ones (85·8 % ulnar loops, 9·6 % whorls, and 3·2 % arches). Cases with *XXX* chromosome constitution did not differ from the controls. The case with *XXXX* sex chromosomes had five arches and five ulnar loops of very low ridge count (total finger ridge count 22). Other defectives had 61·5 % ulnar loops, 24 % whorls, 11·6 % arches and 2·9 % radial loops.

These observations show that certain types of mental deficiency are associated with unusual finger ridge pattern frequencies.

DEMONSTRATIONS

Light microscopy of the statocyst of *Octopus*. By J. Z. YOUNG. *University College London*

There are remarkable parallels with the vertebrate inner ear. The statocyst is a sack filled with endolymph and suspended in perilymph. It contains three sets of receptors:

(1) A verical macula carrying a calcareous otolith.

(2) A ridge, the crista, running in three planes, at right angles, each with its own nerve. The cells of the ridge carry long, loaded hairs and probably serve to signal angular accelerations. There are several sets of hairs asymmetrically arranged, presumably to signal differentially for up/down or right/left acceleration. The nerve fibres of the crista are large (up to 22 μm in diameter).

(3) The membranous wall of the sack contains hair cells of unknown function. They may be pressure receptors recording pressure changes within the body and perhaps preventing the octopus from pulling the body through narrow cracks. The animals are not sensitive to sound.

Muscle tension relationships in *Galago senegalensis*. By E. C. B. HALL CRAGGS, *University College London*

In a study of the jump of *Galago senegalensis* it was calculated that the forces exerted by the two muscle groups quadriceps femoris and triceps surae were of the same order. In view of the fact that the wet weight of triceps surae was never found to exceed 17 % of

quadriceps femoris further investigation was undertaken in an attempt to explain this. Scale diagrams prepared of the musculo-skeletal system of the leg indicated that because of its 'two-joint' arrangement the action of triceps surae must be antagonized at the knee by quadriceps femoris in the action of making the jump. The combination of extension at the knee joint and plantar flexion at the ankle joint entailed in the action also meant that to produce a full range of movement at the ankle joint triceps surae needed to shorten by a much smaller percentage of its length than quadriceps femoris. An investigation of length-tension relationships in these two muscles showed how much this situation was to the advantage of triceps surae, for the minimum tension that it exerted over the range of shortening required was not found to fall below 60% of the maximum, while that of quadriceps femoris dropped to the region of 10%. The muscle fibre length necessary to produce the greater range of shortening in quadriceps femoris also meant that its relative fascicular cross-sectional area/g of dry muscle which is directly related to tension developed, was approximately half that of triceps surae.

Comparative study of the vertebrate olfactory receptors.
By P. GRAZIADEI. *University College London*

Olfactory epithelium of frog, cat and mole was examined with the electron microscope. Bipolar neurons, the olfactory receptors, supporting and basal epithelial cells can be recognized because of their shape, sizes and ultrastructure. Species differences can be observed both in the structure of the neurons and in the number of cilia they bear, and in the structure of supporting cells. Moreover, dendrite, perikaryon and centripetal processes in the olfactory receptors show a quite specific pattern of organelles which may possibly be related to the function of these different parts of the neuron.

Supporting cells show characteristic differences in the different species both in the structure of their cytoplasm and in the structure of their free surfaces. The present observations demonstrate that the cytoplasm of supporting cells has a very complex structure and is richly provided with organelles (mitochondria, free ribosomes, endoplasmic reticulum, etc.). Secretory granules observed in these cells show the morphological phases of the secretory process, with the release of the granules at the surface of the olfactory mucosa. The ultrastructural details of the supporting cells strongly suggest that the role of these cells is more complex than their name implies.

Bowman's glands lying in the connective tissue underneath the epithelium and opening their ducts at the surface of the olfactory epithelium have also been studied with the electron microscope. The presence of microvilli on the free surface of the glandular elements has been demonstrated and the presence of ciliated elements, first described by Dogiel (*Arch. mikrosk Anat.*, 1887) has been confirmed by the present observations with the electron microscope.

Ultrastructure of retinal pigment epithelial cells in the human foetus. By A. S. BREATHNACH and LUCILLE M.-A. WYLLIE. *St Mary's Hospital Medical School.* (Fig. 12)

The demonstration was based upon material obtained from six foetuses ranging in age from 9 to 15 weeks. General features of the cytoplasm of the cells and of their apical, basal, and lateral plasma membranes were illustrated. The manner of development of the pigment granules is essentially similar to that occurring within the epidermal melanocytes. Small, membrane-limited vesicles (probably Golgi) become larger and ovoid in shape, at the same time acquiring a system of concentric internal membranes with an ordered pattern. The resulting premelanosomes (Fig. 12) undergo progressive melanization to become uniformly electron opaque mature melanin granules lacking any evident internal structure.

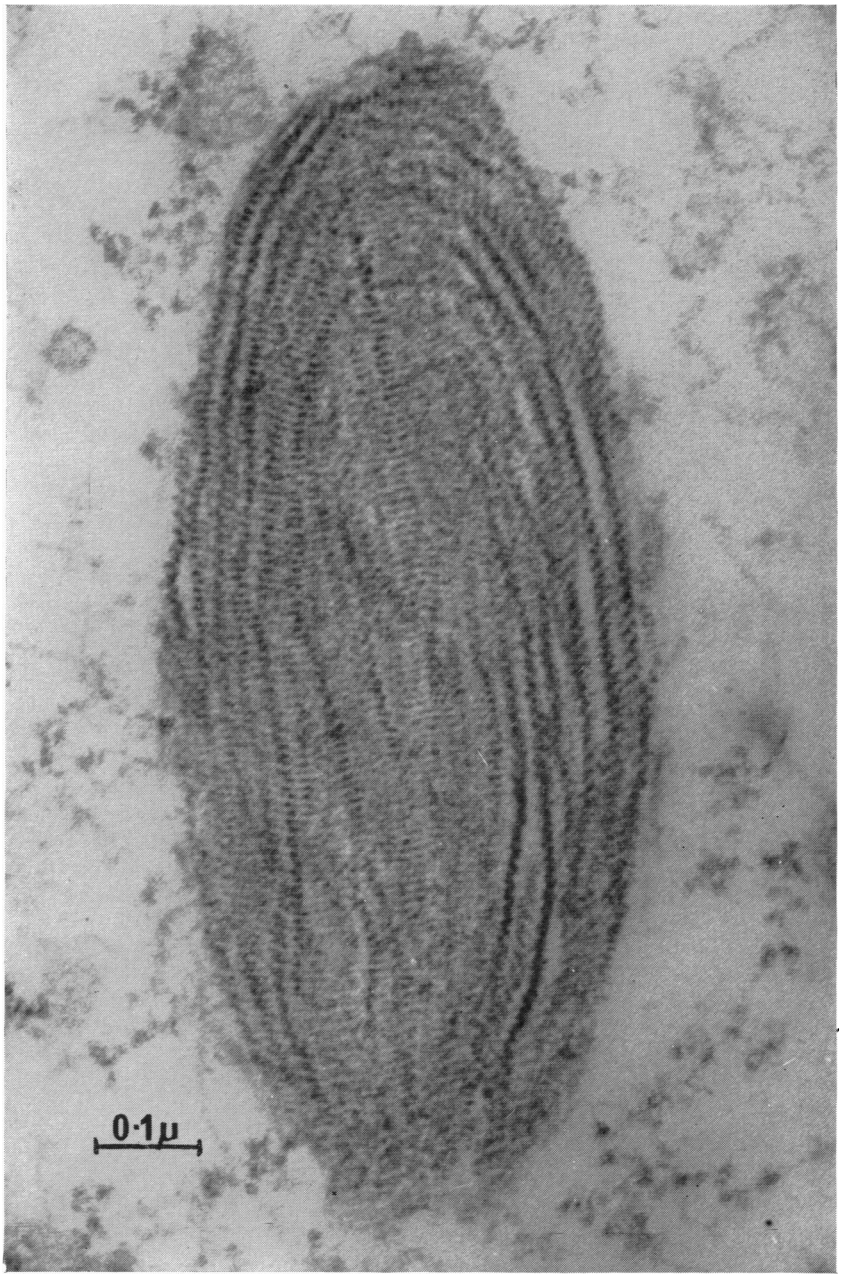

Fig. 12

Lampbrush chromosomes in human oocytes. By T. G. Baker and L. L. Franchi. *University of Birmingham*

It has been suggested that the lampbrush chromosomes seen in the oocytes of various vertebrate and invertebrate species may occur universally in germ cells and probably in somatic cells (e.g. Nebel & Coulon *Chromosoma*, **13**, 1962). These chromosomes have not hitherto been described in 'resting' primordial oocytes in mammals.

The present demonstration of electron micrographs shows the fine structure of chromosomes in the human oocyte at the diplotene stage of meiotic prophase (primordial follicle). The chromosome consists of an axial complex (composed of two or more twisted strands) surrounded by symmetrically arranged fibrillar and granular material. An examination of many micrographs has enabled us to produce a diagrammatic reconstruction of the chromosome. This interpretation of structure, together with observations on histological and squash preparations, is similar to that made by other authors for the lampbrush chromosomes in oocytes in Amphibia.

Neurosecretory pathways from the paraventricular nuclei of the hedgehog. By D. J. Campbell. *University of Birmingham* (Fig 13)

Although fibres of neurosecretory pathways in mammals often show little neurosecretory material at any one time, their demonstration by neurosecretory stains has the advantage over silver methods that the fewer fibres shown may enable tracts to be traced more accurately. The paraventricular neurosecretory pathways in the hedgehog have been studied in serial sections of eight hypothalami, four stained with Gomori's chrome-alum haematoxylin, and four by silver impregnation. The pathways arising from the nucleus paraventricularis (NPV) are shown in Fig. 13A. The ventrolateral tract (VL) (Fig. 13A B) is the most prominent. Most of its fibres pass towards the nucleus supraopticus (NSO), and then mingle with supraoptic fibres; others turn ventromedially before reaching the latter nuclues and pass towards the median eminence. The second largest tract is the lateral (L) whose fibres arise from the triangular division of the nucleus paraventricularis, and pass laterally at right angles to the wall of the third ventricle into the lateral hypothalamic area; some then turn ventromedially and pass dorsal to the nucleus supraopticus towards the median eminence. The ventral tract (V) consists of a few fibres which pass ventrally parallel to the wall of the third ventricle, and are in no part of their course related to the nucleus supra-opticus. Some, but not all specimens, show a fourth pathway, composed of fibres extending dorsally (D) and becoming associated with the rostral poles of the nuclei parataenialis and medialis dorsalis thalami. Such fibres appear to constitute an extra-hypophysial neurosecretory pathway.

The extensive distribution of neurosecretory fibres demonstrated here is an agreement with findings in other mammals (e.g. Laqueur, *J. comp. Neurol.* **101**, 1954; Ford & Kantounis, *J. comp. Neurol.* **108**, 1957). This distribution is clearly of importance not only with regard to functional considerations, but also when interpreting the effects of experimental diencephalic lesions.

A histochemical and quantitative study of cholinesterases in the intraorbital gland of the domestic duck. By Julia Fourman and B. Ballantyne. *University of Leeds*

The intra-orbital gland is a compound tubular gland. In the domestic duck it is large, as in marine birds, the main duct opening under the nictitating membrane.

Cholinesterase activity has been demonstrated in cryostat sections, 20 μm in thickness, by the method of Coupland and Holmes, using acetylthiocholine iodide and butyrylthiocholine iodide as substrates, and 10^{-5} M eserine, 10^{-5} M 62C47h di-iodide and 2×10^{-5} M, *N*, *N*-di-isopropylphosphorodiamidic fluoride as differential inhibitors. With Tris/HCl

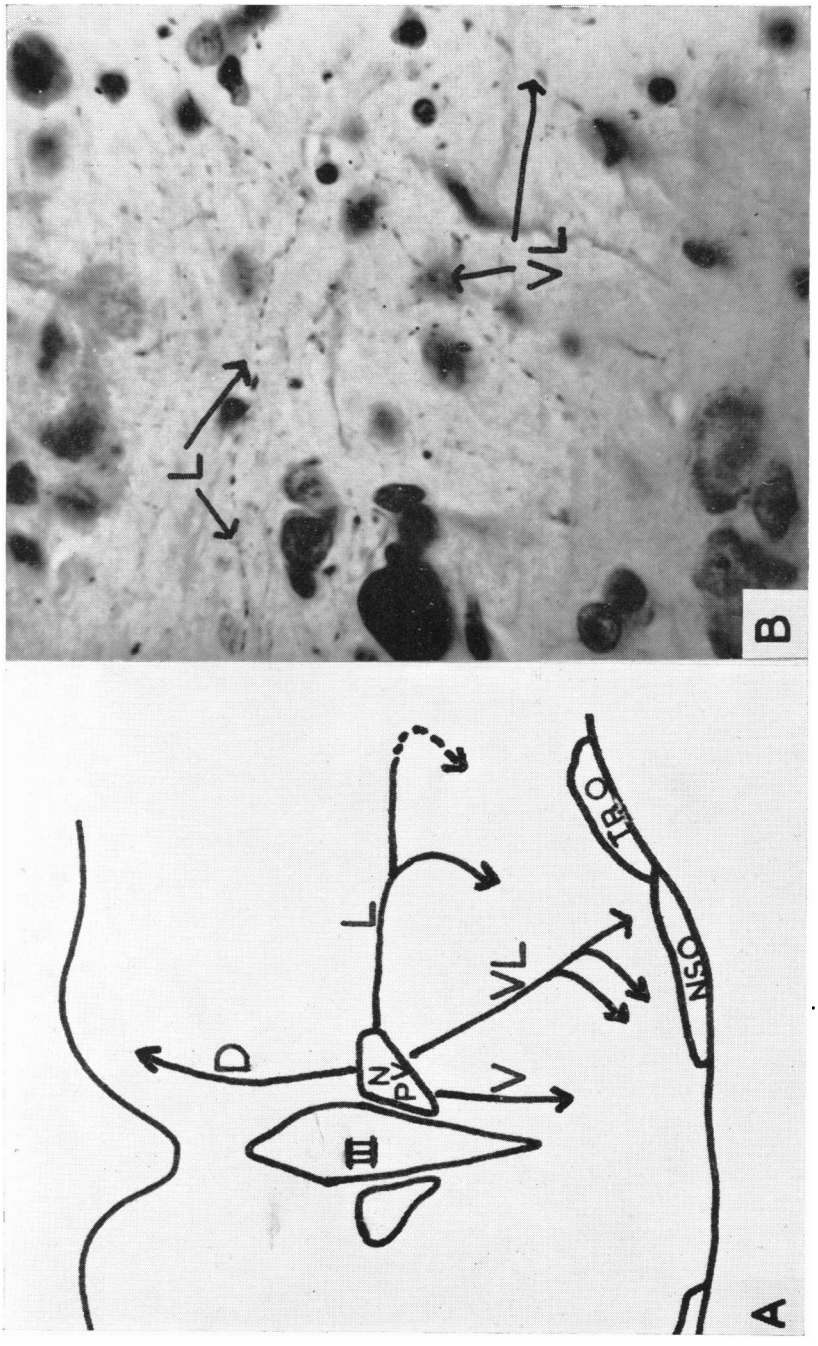

Fig. 13

and acetate buffer systems the optimum incubation time and substrate pH value are 2–4 h and 5·5 respectively for both acetylcholinesterase and butyrylcholinesterase. Fibres with acetylcholinesterase activity have been demonstrated in the interlobular septa and in the connective tissue surrounding the interlobular ducts. Fibres with a similar distribution can be demonstrated with the Holmes silver technique, suggesting that the enzyme is present in nerve fibres. Butyrylcholinesterase is present in the epithelial cells in the proximal parts of the ducts. The intensity of the acetylcholinesterase activity in the fibres was similar in all sections, whereas the histochemical levels of butyrylcholinesterase showed marked variations in the material from different animals.

Cholinesterase activity was measured by continuous electrometric titration at pH 7·4. The mean concentration of acetylcholinesterase in the gland is 68·2 μM/g/h (range 65·5–72·7 μM/g/h), and for butyrylcholinesterase 42·5 μM/g/h (range 20·4–58·7 μM/g/h). The relatively constant value for acetylcholinesterase is in keeping with its presence in nerve fibres, the wide range of butyrylcholinesterase activity is probably related to variations in cellular activity. We have found a close correlation between the subjective assessment of cholinesterase activity based on histochemical techniques and the amount quantitatively measured.

Distribution of cholinesterase in mammalian liver. By BRYAN BALLANTYNE. *University of Leeds.* (Figs 14, 15)

Histochemical techniques for the demonstration of acetyl and butyrylcholinesterase have been used to study the distribution of these enzymes in the liver of adult male Flemish Giant rabbits. In some animals the intrahepatic vascular system was outlined by perfusion with 2% Berlin blue, and in others the Kupffer cells demonstrated by *intra-vitam* indian ink.

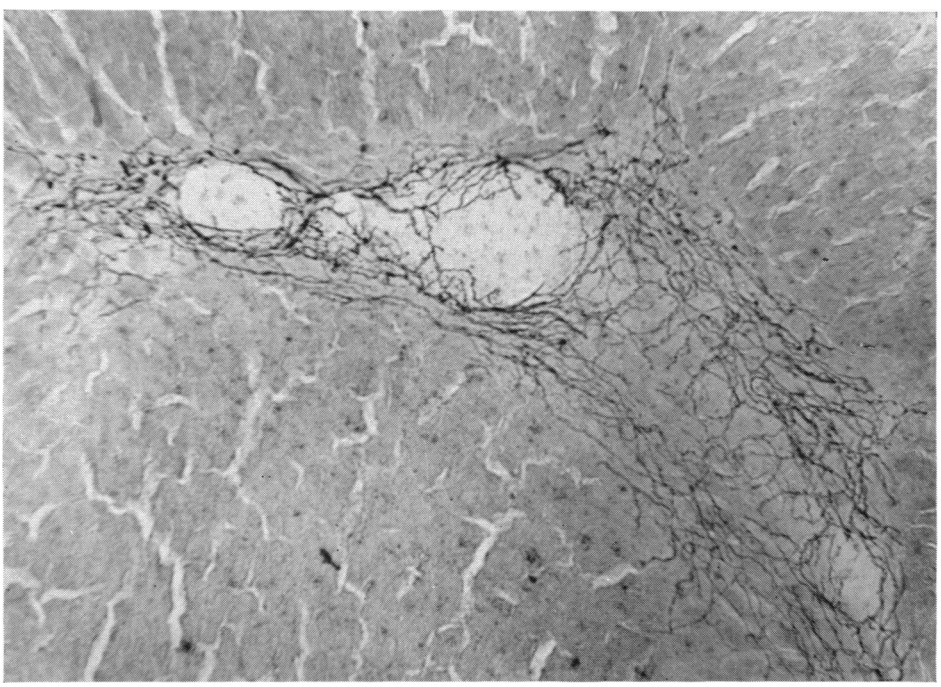

Fig. 14

The intrinsic hepatic nerves contain only butyrylcholinesterase, whose optimum histochemical pH is 5·4. Nerve trunks in each portal tract give branches to plexuses around the portal vein and hepatic artery, and to a general portal plexus which is continuous with adjacent interlobular plexuses (Fig. 14). Nerves to the bile ducts arise from the general portal plexus, and become closely related to the duct epithelium. Intra-hepatic ganglia occur in this species, but there is no parenchymal plexus. The hepatocytes give a positive cytoplasmic reaction for butyrylcholinesterase, which is most intense in centri-lobular cells.

Acetylcholinesterase, with an optimum histochemical pH of 5·5, occurs only in cells lining the sinusoids of hexagonal lobules, the reaction being limited to the centri- and mid-lobular cells (Fig. 15). Material from animals injected with indian ink shows that the enzyme is present in the phagocytic reticulo-endothelial cells of the sinusoids.

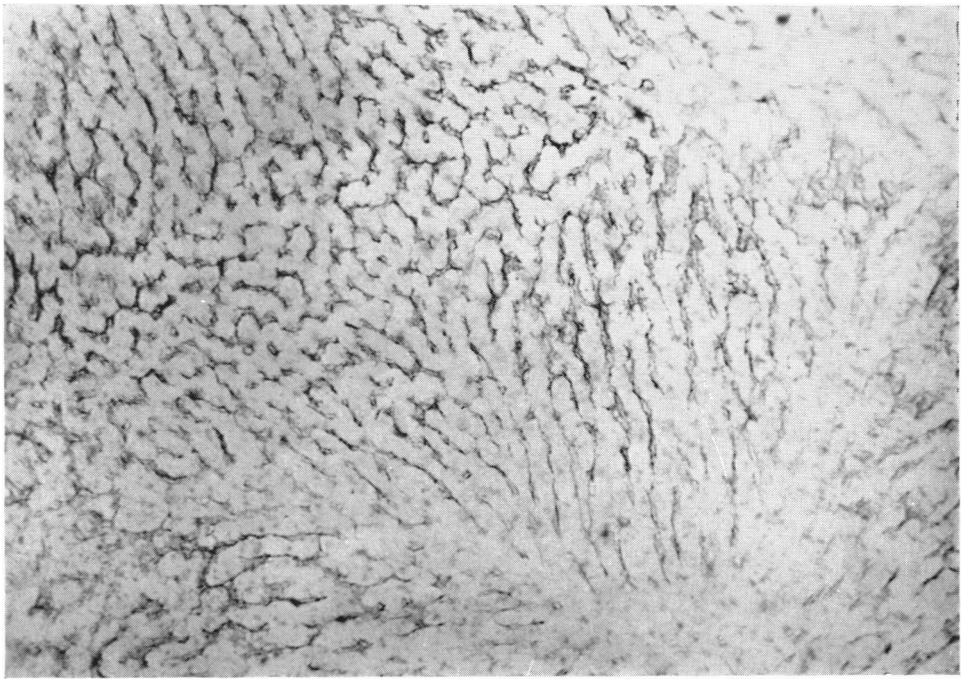

Fig. 15

It is suggested that the butyrylcholinesterase in parenchymal cells is probably concerned in the hydrolysis of potentially toxic esters produced during lipid metabolism in hepatocytes, and that the acetylcholinesterase in the reticulo-endothelial cells plays some general role in the metabolism of lipids and esters, and in detoxification following phagocytosis. The intrinsic hepatic nerves regulate blood flow through the organ, and are probably sensory to the bile ducts.

Carbon replica study of ameloblast-enamel interface. By A. Boyde.
The London Hospital Medical College

The use of a Hilger and Watts 'Stereometer' to make contour maps from stereo-pair electron-micrographs of carbon replicas was shown.

Calibration of tilt cartridges for Siemens Elmiskop 1. By A. BOYDE and R. WILLIS.
The London Hospital Medical College and University College, London

The thickness of an 'ultra-thin' section, or any height difference within any (reasonably thin) specimen, may be calculated from parallax measurements of stereo-pair electron-micrographs. The parallax measurements may be made with simple photogrammetric instruments. The Hilger and Watts 'Stereometer' has proved very suitable for this purpose. It is however necessary to measure accurately the angle through which the specimen was tilted between the two exposures constituting the stereo-pair. The specimen stage and tilting mechanism of the Siemens Elmiskop 1 can be completely removed so that the conditions in the E/M can be emulated outside it. A light beam is reflected from a small fragment of silvered cover-slip (mirror) attached to the head of the tilt cartridge under calibration, to give a large optical level magnification of the tilt. The positions of the reflected light beam through the range of the stereo-probe drive screw are marked on a distant wall. The specimen stage plus tilt cartridge array is then replaced by a sextant, the sextant mirror being placed in exactly the same plane. The tilt angles can then be read directly. Graphs showing the performance of a standard tilt cartridge for the Siemens Elmiskop (tilt range 8° 40′), a Washington-Fearnhead tilt device (tilt range 67°), and a Valdré cartridge (tilt range 45°) was displayed. The Siemens cartridge is suited to the study of thick specimens, e.g. replicas of rough surfaces with height differences in the range 1 to 10 μm. The Washington-Fearnhead and Valdré devices are more suited to high tilt-angle stereo-microscopy to give exaggerated and therefore more easily measurable parallax values with ultra-thin sections.